Anais do
62º Congresso Brasileiro do Concreto
CBC2020
Setembro / 2020

@ 2020 - IBRACON - ISSN 2175-8182

IBRACON

Numerical analysis of the influence of EDCC in reinforcing structural masonry walls

Veronese, Renato B. A. (1); Parsekian, Guilherme A. (2); Shrive, Nigel G. (3)

(1) Student, Masters, Postgraduate Program of Civil Engineering (PPGECiv), Federal University of São Carlos (UFSCar)
(2) Professor, PhD, Department of Civil Engineering, Federal University of São Carlos (UFSCar)
(3) Professor, PhD, Department of Civil Engineering, University of Calgary
Mail Address: renatobaiochi@gmail.com

Abstract

The purpose of this work is to evaluate the behavior of structural masonry walls reinforced with a sustainable cementitious coating, called Eco-friendly Ductile Cementitious Composite (EDCC), subject to compression, through finite element modeling of previous experimental tests. The main objective is to validate a numerical model that correctly simulates the compression test on a small masonry wall, so that a parametric study can be executed subsequently to assess the influence of several associated variables. A literature review has been completed about the parameters that need to be defined for the component materials and interfaces and the strategies that can be implemented in order to model structural masonry walls accurately with the finite element method. Subsequently, the model was calibrated, comparing the results of stress vs. strain diagrams of the experimental tests with the numerical simulations performed by other authors, in order to establish parameters common to the results and to substantiate analysis of the behavior of the walls.

Anais do
62º Congresso Brasileiro do Concreto
CBC2020
Setembro / 2020

1 Introduction

There are several techniques available to reinforce and repair masonry structures in order to avoid damage related to lateral actions. Among these techniques, there are the methods of grout injection, the application of polymeric fibers or coating with different types of mortars (reinforced or not, executed manually or with projection equipment). It is important to note that the first technique presented has execution limits. In the case of reinforcement systems applied to coatings and composed of polymeric fibers, there is a possibility of cost reduction. However, these systems are generally not particularly ecologically friendly, especially if the coatings require high levels of cement in their composition (LI et al. (2017)).

As a result, more sustainable technologies for reinforcing and repairing masonry panels have emerged in recent years, related to the use of waste in the composition of the materials used. Some researchers propose sustainable methods, such as mortar coatings with a lower cement content in their composition (LI et al. (2017); SOUDAIS et al. (2017)), and that is the type of material used to accomplish the work described herein.

In addition to the material issues, numerical modeling has been used for many years to analyze all sorts of structures. With numerical modeling, it is possible to calibrate the material behavior so the model correctly simulates certain tests and to change some factors later, such as the scale of a structure, to make a complete study of the micro parts of a structure that cannot be analyzed in experimental tests.

Therefore, the objective of this work is to model the compression tests on unreinforced concrete masonry and masonry coated with an Eco-friendly Ductile Cementitious Composite (EDCC), described by Parsekian and Shrive (2019), and to adjust the parameters such that the tests are correctly simulated. Attaining this objective will enable future studies on numerical modeling on EDCC coated masonry.

2 Framework

2.1 Eco-friendly Ductile Cementious Composite (EDCC)

Eco-friendly Ductile Cementitious Composite (EDCC) is cementitious composite developed and studied over the last eight years, consisting in a mix of Portland cement, fly ash, sand, silica fume and PVA and PET fibers. The proportion of fly ash (coal industry waste) is about 70% of the total binder in the mixture, defining the material as eco-friendly. EDCC was developed at University of British Columbia to work as a new repair material, (YAN (2016); DU (2016)).

@ 2020 - IBRACON - ISSN 2175-8182

Li et al. (2017) tested EDCC and obtained a compression strength at 56 days of 48.4 MPa, with an elastic modulus of 16.0 GPa (indicating this material is approximately twice as deformable as a regular C45 concrete) and a splitting tensile strength of 6.3 MPa. Subsequently, Parsekian and Shrive (2019) performed compression, flexural and shear tests on concrete masonry walls strengthened with an EDCC coating on both sides (faces), and a summary of the compression test results is presented in Table 1. The walls were unreinforced (URW) or had 5, 10 or 20 mm EDCC coatings.

Table 1 – Comparison of compression test results (Adapted from PARSEKIAN; SHRIVE, 2019).

Block faceshell thickness [mm]	35.8	35.8	35.8	35.8
EDCC thickness [mm]	0	5	10	20
Failure load – experimental result average [kN]	968	1051	1195	1391
Failure stress – experimental result average [MPa]	17.1	16.3	16.5	15.8
Estimated EDCC stress at wall failure [MPa]	-	13.42	13.42	13.42
Calculated EDCC strain (‰)	0.00	0.84	0.84	0.84
Calculated failure load – masonry component [kN]	968	968	968	968
Estimated masonry stress at wall failure [MPa]	17.11	17.11	17.11	17.11
Calculated failure load – EDCC component [kN]	0	106	212	424
Calculated masonry strain (‰)	1.04	1.04	1.04	1.04
Calculated failure load – total [kN]	968	1074	1180	1392
Calculated / experimental failure load	100%	102%	99%	100%

It can be seen that while the failure stress decreases with increasing EDCC coating thickness, the failure load increases. In addition, the authors estimated values of EDCC failure stress and strain, and then compared their estimations to the graph (Figure 1) generated in the tests by the LVDTs installed on the face of the walls. They concluded that the strain deformation at failure for the 5 and 10 mm thick EDCC-walls was very close to 0.84‰ (value calculated from materials properties), noticing that this deformation is below the maximum deformation of unreinforced walls. However, the 20 mm thick EDCC-wall showed a more ductile behavior and presented the failure at a higher deformation value (PARSEKIAN; SHRIVE (2019)).

Figure 1 – Stress vs strain curves for unreinforced and coated walls (PARSEKIAN; SHRIVE, 2019).

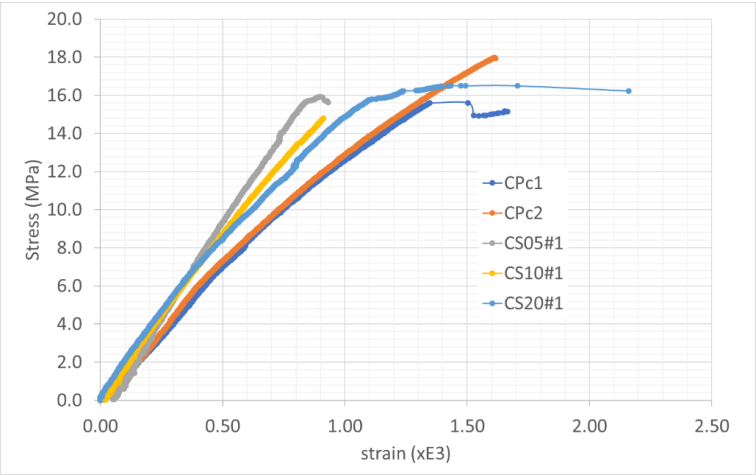

@ 2020 - IBRACON - ISSN 2175-8182

2.2 Masonry compression behavior

The main stress type that masonry walls are subjected to is related to compression. The determination of compressive strength of a wall made with concrete blocks, according to standard NBR 16522 (ABNT, 2016), can be performed on a real wall, a small wall and/or a prism.

First, there is the compressive strength test on a full-scale wall, as shown in Figure 2a. The test specimen consists of a wall 260 cm high and 120 cm wide, with thickness defined by the block used. Then a distributed load is applied on the top of the wall and increased to wall failure.

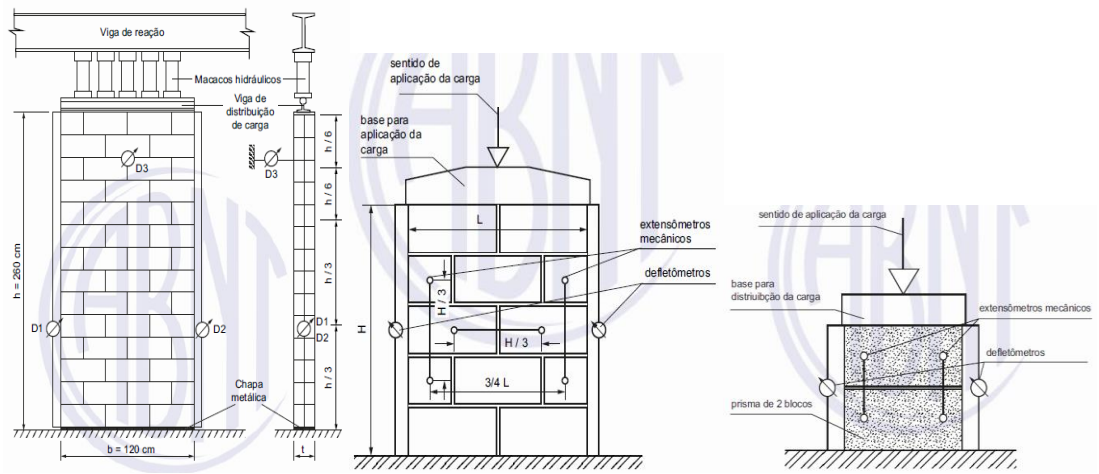

(a) Full-scale wall. (b) Small wall. (c) Prism.

Figure 2 – Test types for determining compressive strength in masonry walls (ABNT (2016)).

The next test consists of a small wall resistance test, with a wall five courses high and two units long, as illustrated in Figure 2b. A distributed force is applied at the top of the structure, similar to the process mentioned above, until total rupture of the wall.

Finally, and more simple, there is the test performed on prisms formed with two blocks, as shown in Figure 2c. The blocks are properly arranged, with transducers fixed on their faces, and then a distributed force is applied to the top until total rupture of the prism.

It is possible to observe in literature that some authors, such as Francis et al. (1970), Hilsdorf (1969), Brown and Whitlock (1982), Atkinson et al. (1985), Hamid and Drysdale (1979), Khoo and Hendry (1973) and Shrive (1983), performed tests on prisms, trying to explain the failure mechanism and predict the masonry's compressive strength. In situations where the compressive strength of the mortar used is lower than strength of the block, it is possible to see rupture close to the joint (most common case), as shown in Figure 3a. For situations in which the block has lower compressive strength than the

mortar, it is possible to observe the block crushing before the mortar joint breaks, as seen in Figure 3b.

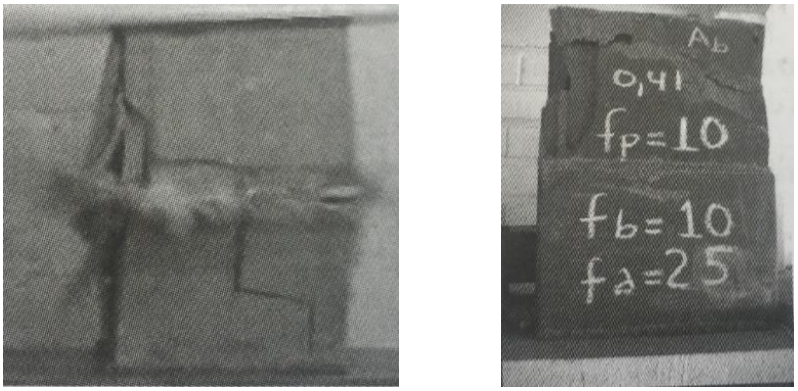

(a) Mortar weaker than block. (b) Mortar stronger than block.
Figure 3 – Different types of prisms failure (PARSEKIAN; HAMID; DRYSDALE (2014)).

In Figure 4, there are results of experimental tests performed on three-block hollow concrete prisms, showing a crack along the entire lateral height of the wall. This is a common crack model in prisms or in structural masonry walls where there are only partial mortar application, when submitted by compression forces, as presented by Santos *et al.* (2017) and Oliveira (2014).

(a) (b)
Figure 4 – Three block prism failure ((a) SANTOS *et al*. (2017)); (b) OLIVEIRA (2014).

2.3 Numerical modeling

A way to study the isolated effect of each parameter on the overall behavior of a structure is to use numerical modeling based on finite element modeling. Numerical analysis presents some advantages over experimental testing, since it is a less expensive way for

conducting research rather than testing specimens. In addition, numerical modeling allows study of the most influential parameters that can affect the behavior of masonry walls. However, the correct calibration must be done in order to validate and compare the model output with the experimental results.

Finite element modeling simulates a heterogeneous structure by dividing it into small elements, in order to calculate the reactions and deformations in each element created. The shape function of a displacement-based element defines how it will deform, and the element stiffness is determined by integrating numerically a function of the differential of the shape function and the constitutive properties assigned to the element. Elements can be classified in many different types. In the case of solid structures, the elements will be 3D, preferably with cube shapes. Each element contains nodes and compatibility is required for all elements associated with that node, but the nodes that will be analyzed depend on which type of integration will be considered (complete or reduced) and the shape function degree (linear or quadratic). Therefore, the accuracy and precision of the results of a model will be heavily influenced by the choices made before the model is processed; in general, the more nodes in a model, the more accurate the results will be.

The choice of material and interface properties for the modelling are critical, so those used here are presented next.

2.3.1 Concrete Damage Plasticity (CDP)

Concrete Damage Plasticity (CDP) is a formulation for modelling the behavior of concrete-like materials inside the Materials tool in ABAQUS. Various parameters need to be defined for correct simulation of the material of interest. These parameters are responsible for allowing the expansion of the constitutive equations of the material (in this case, concrete) from the uniaxial state to a multiaxial state (AGUIAR (2015)). These parameters are explained below:

- Dilation angle (Ψ): According to Cardoso (2014), the dilation angle is related to the inclination that the plastic potential can reach under high confinement stresses, or more simply, the friction angle of the concrete in a Coulomb or Mohr-Coulomb definition of shear strength;

- Eccentricity: The eccentricity can have values of 0 or 0.1, depending on the shape of the yield surface in the meridian plane, with 0 being for a straight line and 0.1 for the hyperbolic shape (Drucker Prager theory);

- f_{b0}/f_{c0}: This parameter defines the ratio between the yield stresses in the biaxial and uniaxial states, with the default value being 1.16 (SANTOS et al. (2017));

- K: The K parameter can be defined as the relationship between the distances from the hydrostatic axis and the traction and compression meridians in the cross section

@ 2020 - IBRACON - ISSN 2175-8182

of the studied part. ABAQUS recommends the default value of 0.6667 for this parameter (MEDEIROS (2018));

- Viscosity parameter: The main function of the viscosity parameter is to facilitate the convergence process of numerical models, admitting viscosity in equations that constitute the model's processing (SANTOS et al. (2017)).

In addition to the parameters related to plasticity damage of concrete, the compression and tensile behavior in the inelastic domain of the material must be defined. Finally, it is necessary to define the parameters of material damage in the inelastic domain for the two behaviors, where they indicate the appearance and progression of cracking.

2.3.2 Interfaces

For the construction of structural masonry models in ABAQUS, Santos *et al.* (2017) used four types of interactions in the Interactions tool: Normal behavior, Tangential behavior, Cohesive behavior and Damage evolution. These interactions are:

- Normal behavior: Hard contact within this option prevents one surface from penetrating another as soon as they contact and allows separation of the surfaces with no load as they move apart;

- Tangential behavior: this contact simulates the friction between the surfaces, being defined mainly by the coefficient of static friction: in addition there is the possibility of imposing a shear stress limit for the connection, as seen in Figure 5;

- Cohesive behavior: this interaction works as a type of glue, where it is possible to specify the normal and tangential stiffness of the interface;

- Damage evolution: this interaction is associated with Cohesive behavior, where it is possible to define degradation of that behavior through a coefficient related to fracture evolution at the interface.

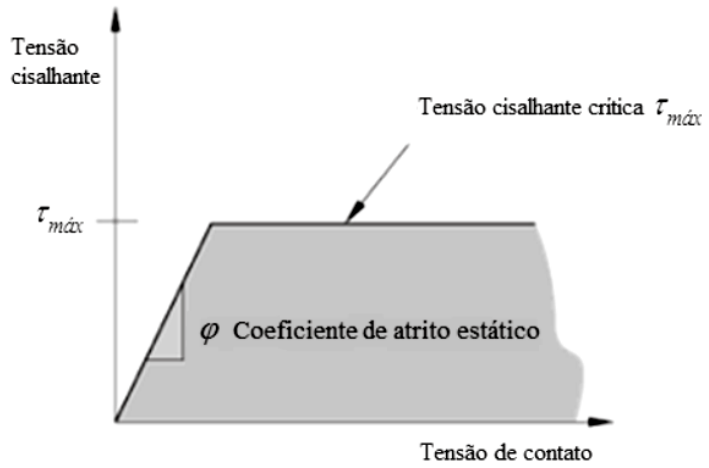

Figure 5 – Tangential behavior (SANTOS et al. (2017)).

From the defined parameters, the surfaces that need some type of connection are selected. In addition to the main connections, which would be the interfaces between blocks and mortar and between the EDCC coating and the wall face, connections between the walls of the blocks (divided in half) should also be considered, because it is a region where many cracks form, as shown in Figure 4. Next, each type of connection and its main characteristics will be explained.

3 Methodology

3.1 Materials

In order to achieve the main objective of this work, the results obtained by Parsekian and Shrive (2019) concerning compression tests in unreinforced and coated masonry walls were analyzed. Four different tests were modelled with ABAQUS: the reference test with URW; and three tests with EDCC coatings of 5, 10 and 20 mm thickness on both sides of the wall. In Figure 6(a) the compression test scheme is shown and an example of a final failure obtained by Parsekian and Shrive (2019) may be seen in Figure 6(b).

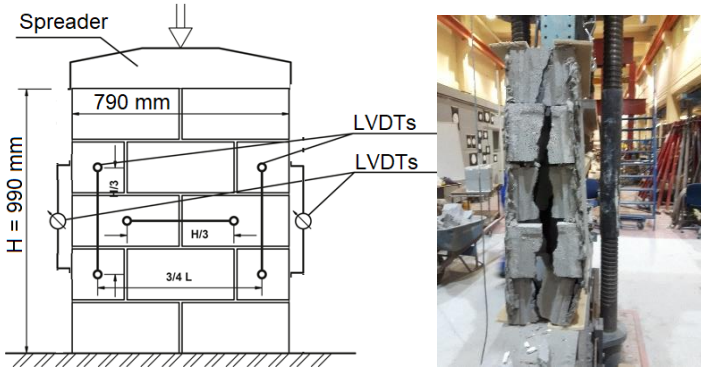

(a) (b)

Figure 6 – Compression test scheme and total failure (PARSEKIAN; SHRIVE (2019)).

3.2 Model description

According to Bolhassani (2015) and Medeiros (2018), when working with masonry walls in ABAQUS, it is possible to consider just one material for the wall. They considered just the

@ 2020 - IBRACON - ISSN 2175-8182

concrete blocks (nominally 20 cm high and 40 cm wide), disregarding the mortar joints. So, following that approach, two 3D deformable parts, as shown in Figure 7, were created, considering 2 different types of blocks, 19 and 39 cm.

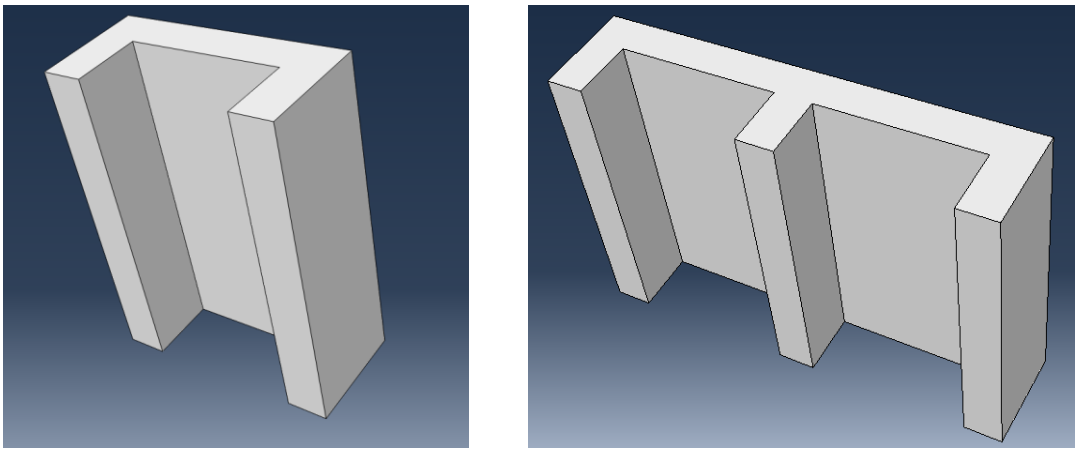

a) 19 cm block b) 39 cm block

Figure 7 – Half blocks made in ABAQUS.

For this configuration, the element type for the mesh was defined as being preferably square, with C3D20 elements (solid element with twenty nodes, quadratic shape function (considering nodes between the vertex nodes) and complete integration) 50 mm wide. This type of element was chosen due to the greater precision in results, but the mesh width could not be smaller than 50 mm because of the time demand to process the models. In Figure 8, the mesh layouts are shown for the four small walls modelled, as per the geometry of the experimental walls, showing all the parts connected together.

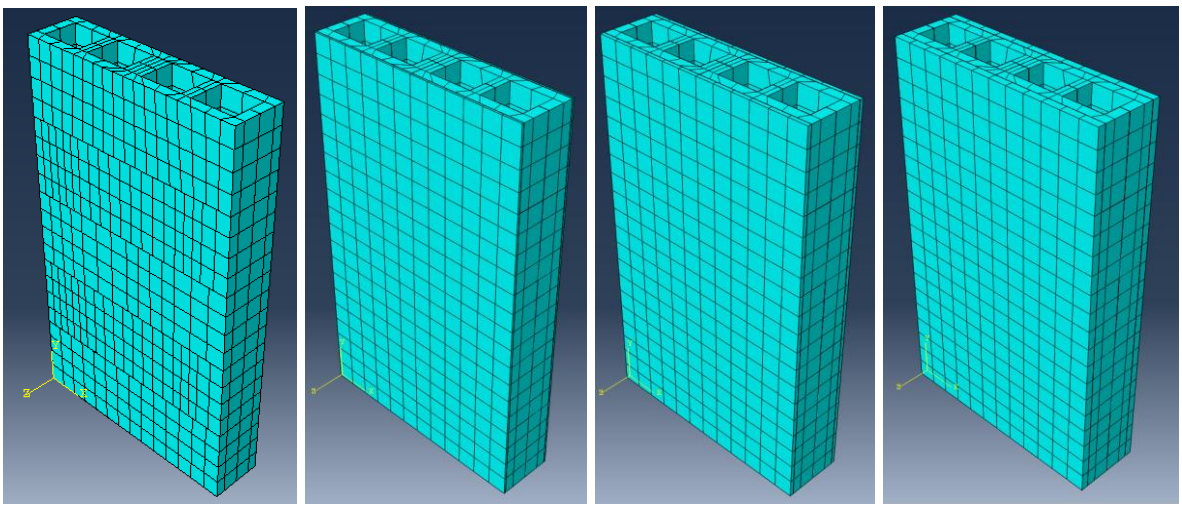

a) URW b) 5mm coated c) 10mm coated d) 20mm coated

Figure 8 – Small meshed masonry walls.

3.3 Constitutive model

For this work, the simplification was used of defining only one material for the entire concrete block wall, following the approach of MEDEIROS (2018) and BOLHASSANI (2015), with the blocks being connected without mortar joints. Values for the various parameters which needed to be specified were based on the results from both those authors and Parsekian and Shrive (2019), but with some adjustment to obtain good model calibration. The parameters used to create the material, both for the elastic and plastic (CDP) regimes are listed in Table 2. The compression and tensile behaviors of the material, respectively, in addition to damage parameters (D_c and D_t) for both behaviors are presented in Tables 3 and 4. Note that the behaviors in plastic domain presented in the last tables are mainly due to stress (σ_v) and inelastic strain (ε_{inel}).

Table 2 – Elastic and CDP parameters (Adapted from PARSEKIAN; SHRIVE (2019)).

Material	Elasticity		Plasticity				
	E (GPa)	ν	Ψ	€	f_{b0}/f_{c0}	K	Visc.
Masonry	16.5	0.19	32	0.1	1.16	0.6667	0.01
EDCC	16.0	0.21	32	0.1	1.16	0.6667	0.01

Table 3 – Material compression behavior (with damage) (Adapted from MEDEIROS (2018)).

σ_v (MPa)	ε_{inel}	D_c
0.59	0	0
1.56	0.0001	0
1.99	0.0005	0
0.66	0.0046	0.6649
0.32	0.0077	0.8408
0.20	0.0105	0.8989
0.15	0.0132	0.9266
0.11	0.0159	0.9425

Table 4 – Material tensile behavior (with damage) (Adapted from MEDEIROS (2018)).

σ_v (MPa)	ε_{inel}	D_t
0.0400	0	0
0.0114	0.00008	0.7143
0.0062	0.00013	0.8441
0.0044	0.00018	0.8900
0.0035	0.00022	0.9134
0.0029	0.00027	0.9278

@ 2020 - IBRACON - ISSN 2175-8182

3.4 Interfaces description

As discussed in section 2.3.2, there are three types of interface in the modelling of the tests on the masonry walls with EDCC coatings: between the internal interfaces of the blocks; between the EDCC coating and the masonry; and between the blocks and the mortar. As there are no mortar joints in the model, the interface between the blocks and the mortar was taken as being between the blocks, both vertically and horizontally. For both interfaces the Normal, Cohesive and Damage Evolution parameters need to be defined. In addition, the Tangential Behavior for the interfaces between the blocks and between the EDCC coating and the masonry wall was specified. The values used to create the two interfaces that do not include EDCC coating are shown in Table 5.

Table 5 – Interfaces parameters (BOLHASSANI (2015)).

Tangential behavior	Normal behavior	Cohesive behavior (MN/m)			Damage initiation (MPa)			Damage evolution
φ	Hard Contact	K_{nn}	K_{ss}	K_{tt}	Normal	Shear 1	Shear 2	Displ. (mm)
0.78		8.7	8.7	0	12.6	0.21	0	2.0

According to Bolhassani (2015), the tangential behavior is defined by Coulomb friction, characterized by a friction coefficient, in this case 0.78 for this kind of structure. It is possible to define a limit for shear stress, such that when this limit is reached, tangential motion begins in the structure. This limit is calculated by multiplying the coefficient of friction (μ) and the contact pressure between the two surfaces (ρ) (Equation 1).

$$\tau_{máx} = \mu\rho \quad \text{(Equation 1)}$$

Cohesive behavior and damage initiation are related to the stiffness and the direct resistance between two surfaces, respectively. Both include normal and shear resistance, that can be determined in experimental wall tests. In Table 6 the calculated parameters for the interaction between the EDCC coating and the wall surface are listed. Some of the parameters are results from the experimental tests conducted by Parsekian and Shrive (2019) on EDCC coated walls, shown in Table 7, as for example, the damage initiation parameters and the limit shear stress in tangential behavior.

Table 6 – Interface parameters between EDCC coating and masonry surface.

Tangential behavior		Cohesive behavior (MN/m)			Damage initiation (MPa)			Damage evolution
φ	$\tau_{máx}$ (MPa)	K_{nn}	K_{ss}	K_{tt}	Normal	Shear 1	Shear 2	E_f (Nm)
0.78	0.81	8.7	8.7	0	1.04	0.15	0	50

Table 7 – Pull-off tests results for 56 days (Adapted from PARSEKIAN (2017)).

Number of specimens	AVG (MPa)	STDV (MPa)
18	1.04	0.28

@ 2020 - IBRACON - ISSN 2175-8182

The coefficient of friction was assigned the value of 0.78, but the limit for shear stress was calculated according Equation 1, using 0.78 for the coefficient of friction and 1.04 for contact pressure between the surfaces. The cohesive behavior and damage evolution parameters were defined as in Bolhassani (2015), but values for the damage initiation parameters were taken from the tests on EDCC coated masonry (PARSEKIAN (2017) and PARSEKIAN; SHRIVE (2019)).

4 Results and discussion

The main results analyzed for the different models was related to the maximum failure compressive stress and strain in the small walls, so stress vs strain curves were generated for all four tests modeled, shown in Figure 9. In addition to analysis related to the failure stress, behaviors for compression and tensile damage were also generated at the failure stress point of the tests, in order to compare with the real wall failures. Compression and tensile damage comparison to URW and 5 mm EDCC coated wall are shown in Figures 10 and 11, respectively.

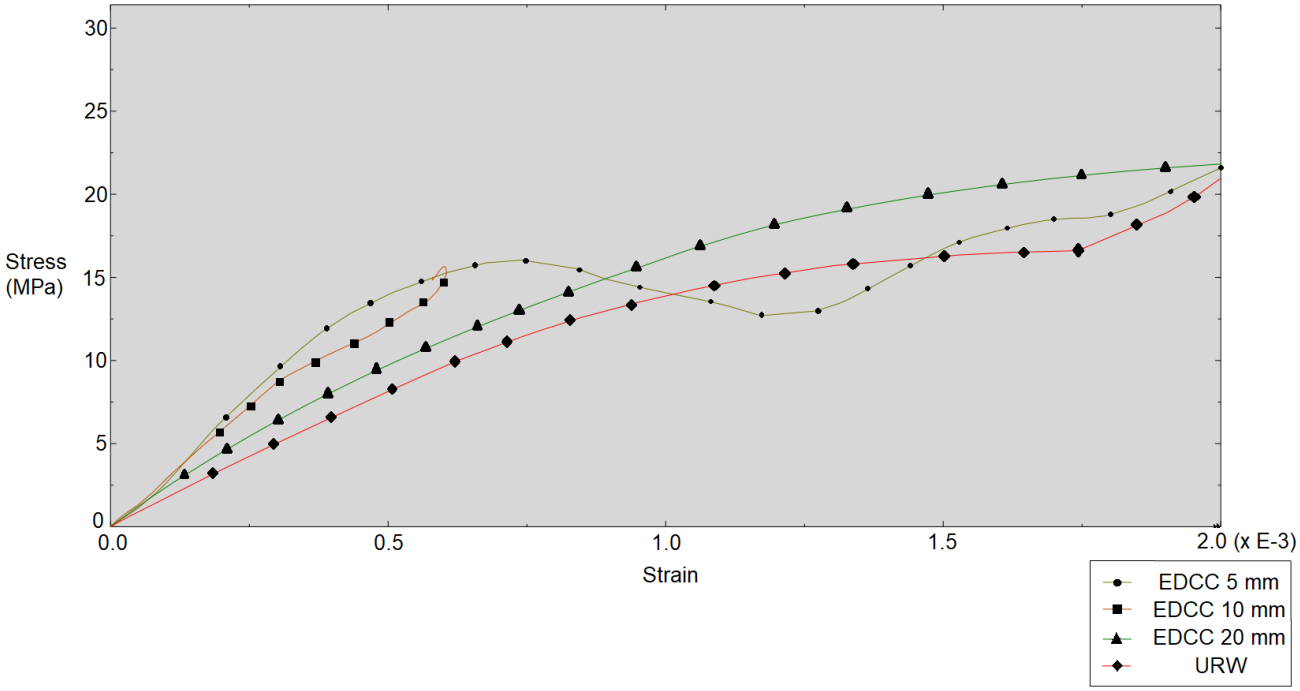

Figure 9 – Stress vs strain curves.

@ 2020 - IBRACON - ISSN 2175-8182

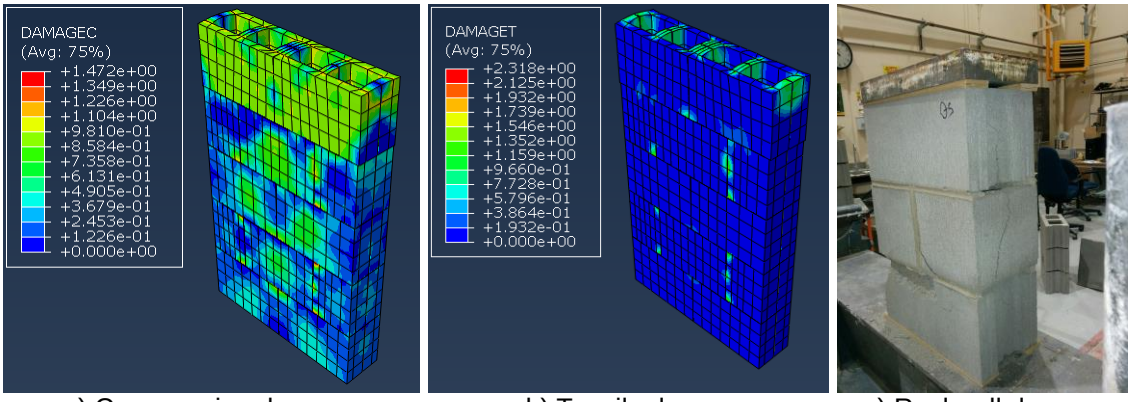

a) Compression damage b) Tensile damage c) Real wall damage (PARSEKIAN; SHRIVE (2019))

Figure 10 – URW damage comparison.

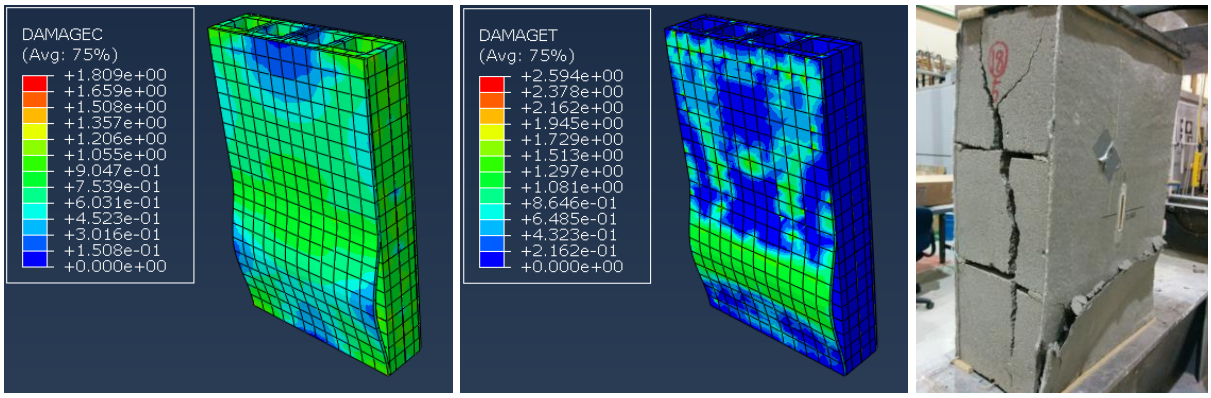

a) Compression damage b) Tensile damage c) Real wall damage (PARSEKIAN; SHRIVE (2019))

Figure 11 – 5 mm EDCC coated wall damage comparison.

It is possible to see in Figure 10 that the URW cracks appear mainly by compression stress in the blocks at the top, spreading down through the wall with cracks showed in the joints and the lateral face of the wall. However, when the EDCC coating is applied on masonry surfaces, the cracks tend to form at the vertices of the wall and in the middle down face of the EDCC coating, showing the failure by adhesion between the surfaces and consequently a tensile stress in the EDCC coating, as shown in Figure 11.

Comparing both results from Parsekian and Shrive (2019) (Figure 1) and those shown in Figure 9, it is possible to observe a similarity between the curves plotted, but with some small differences. The results found in the numerical analysis show that the EDCC coated walls present higher stiffnesses than URW, as happened in the experimental tests. However, the tests with 5 and 10 mm EDCC thickness showed some instability during application of the displacement, but with consistent absolute stress and strain failure values. The stresses at failure for the modeled tests, and the error compared to the results

@ 2020 - IBRACON - ISSN 2175-8182

of the experimental tests obtained by Parsekian and Shrive (2019) are presented in Table 8.

Table 8 – Comparison of compression failure stresses (MPa).

Reference	URW	5 mm EDCC	10 mm EDCC	20 mm EDCC
PARSEKIAN; SHRIVE (2019)	17.1	16.3	16.5	15.8
CURRENT MODELLING	18.2	17.0	16.0	16.5
Error	6.4%	4.3%	-3.0%	4.4%

5 Conclusions

Based on the results, it is possible to conclude that the numerical models were capable of reproducing both the mechanical behavior and the failure modes of the walls. There is a slight difference between the experimental and numerical results, with a maximum error of 6.5% for absolute stress and strain values. This level of error is considered acceptable given the normal variability of masonry, so we conclude that the model and model parameters selected are satisfactory for performing further numerical analyses on full scale walls and even one or more stories. Once those numerical models are calibrated, they will help other researchers to carry on studies about the influence of each variable in the global behavior of masonry elements.

References

AGUIAR, O. P. **Estudo do comportamento de conectores Crestbond em pilares mistos tubulares preenchidos com concreto.** 2015. 230 f. Dissertação (Mestrado) - Escola de Engenharia, Universidade Federal de Minas Gerais, Belo Horizonte, 2015.

ASSOCIAÇÃO BRASILEIRA DE NORMAS TÉCNICAS. **NBR 16522:** Alvenaria de blocos de concreto – Métodos de ensaio. Rio de Janeiro, 2016.

ATKINSON, J. *et al.* A deformation failure theory for stack-bond brick masonry prisms in compression. In: INTERNATIONAL BRICK MASONRY CONFERENCE, 7., 1985, Melbourne. ***Proceedings…*** Melbourne, 1985. p. 577-592.

BOLHASSANI, M. **Improvement of Seismic Performance of Ordinary Reinforced Partially Grouted Concrete Masonry Shear Walls.** PhD. thesis, Drexel University, Philadelphia, PA, USA, 2015.

BROWN, R.; WHITLOCK, A. Compressive strength of grouted hollow brick prisms. In: BORCHELT, J. G. (Ed.). ***Masonry***: materials, properties and performance. Philadelphia: ASTM (STP 778), 1982.

CARDOSO, H. S. **Estudo Teórico-Experimental de Parafusos Utilizados como Dispositivos de Transferência de Carga em Pilares Mistos Tubulares Preenchidos com Concreto.** 2014. 182 f. Dissertação (Mestrado) - Escola de Engenharia, Universidade Federal de Minas Gerais, Belo Horizonte, 2014.

DU, Y. **Durability performance of eco-friendly ductile cementitious composite (EDCC) as a repair material**. MSc thesis, University of British Columbia, Vancouver, BC, Canada, 2016.

FRANCIS, A. J. *et al.* The effect of joint thickness and other factors on the compressive strength of brick-work. In: INTERNATIONAL BRICK MASONRY CONFERENCE, 2., 1970, Stoke-on-Trent. ***Proceedings…*** Stoke-on-Trent, 1970. p. 31-37.

HAMID, A. A.; DRYSDALE, R. G. Suggested failure criteria for grouted concrete masonry under axial compression. **ACI Journal,** v. 76, n. 10, p. 1047-1062, 1979.

HILSDORF, H. K. Investigation into the failure mechanism of brick masonry under axial compression. In: JOHNSON, F. B. (Ed.). ***Designing, engineering and construction with masonry products.*** Houston: Gulf Publishing, 1969. p. 34-41.

KHOO, C. L.; HENDRY, A. W. A failure criterion for brickwork under axial compression. In: INTERNATIONAL BRICK MASONRY CONFERENCE, 3., 1973, Essen. ***Proceedings…*** Essen, 1973. p. 141-145.

LI, R.; PARSEKIAN, G. A.; SHRIVE, N. C. Properties of Eco-friendly Ductile Cementitious Composites (EDCC). In: CONGRESSO BRASILEIRO DE CONCRETO, 59., 2017, Bento Gonçalves. ***Proceedings…*** Bento Gonçalves: IBRACON, 2017.

MEDEIROS, W. A. **Pórticos em concreto pré-moldado preenchidos com alvenaria participante.** 2018. 163 f. Dissertação (Mestrado) – Engenharia Civil, Departamento de Engenharia Civil, Universidade Federal de São Carlos, 2018.

OLIVEIRA, L. M. F. **Estudo teórico e experimental do comportamento das interfaces verticais de paredes interconectadas de alvenaria estrutural.** 2014. 272 f. Tese (Doutorado) – Curso de Engenharia Civil, Escola De Engenharia De São Carlos, Universidade de São Paulo, São Carlos, 2014.

PARSEKIAN, G. A. **RELATÓRIO DE PESQUISA FAPESP 23112.003164/2016-01:** Tecnologia Sustentável para Reabilitação de Alvenarias. São Carlos: Universidade Federal de São Carlos, 2017. 31p.

PARSEKIAN, G. A.; HAMID, A. A.; DRYSDALE, R. G. **Comportamento e dimensionamento de Alvenaria Estrutural.** 2. ed. rev. 1. reimpr. São Carlos: EdUFSCar, 2014. 625 p.

PARSEKIAN, G. A.; SHRIVE, N. G. Preliminary Results on Surface Coating Strengthening Concrete Block Masonry With Eco-Friendly Ductile Cementitious Composite. In: NORTH AMERICAN MASONRY CONFERENCE, 13., 2019, Salt Lake City. ***Proceedings…*** Salt Lake City, 2019.

SANTOS, C. F. R. *et al*. Numerical and experimental evaluation of masonry prisms by finite element method. **Revista IBRACON de Estruturas e Materiais,** [s.l.], v. 10, n. 2, p. 477-508, abr. 2017.

SHRIVE, N. G. A fundamental approach to the fracture of masonry. In: CANADIAN MASONRY SYMPOSIUM, 3., 1983, Edmonton. ***Proceedings…*** Edmonton, 1983. p. 4.1-4.16.

SOUDAIS, P. R. N. *et al.* Strengthening and repair of masonry under compressive load and testing of EDCC-strengthened prisms. In: CANADIAN MASONRY SYMPOSIUM, 13., 2017, Halifax. ***Proceedings…*** Halifax, 2017.

YAN, Y. **Investigation into bond strength between EDCC/Masonry**. MSc thesis, University of British Columbia, Vancouver, BC, Canada, 2016.